# Vanadate Induces Calcium Signaling, $Ca^{2+}$ Release-Activated $Ca^{2+}$ Channel Activation, and Gene Expression in T Lymphocytes and RBL-2H3 Mast Cells Via Thiol Oxidation[1]

**George R. Ehring, Hubert H. Kerschbaum,[2] Christopher M. Fanger, Claudia Eder,[3] Heiko Rauer, and Michael D. Cahalan[4]**

**Using ratiometric $Ca^{2+}$ imaging and patch-clamp measurement of $Ca^{2+}$ channel activity, we investigated $Ca^{2+}$ signaling induced by vanadium compounds in Jurkat T lymphocytes and rat basophilic leukemia cells. In the presence of external $Ca^{2+}$, vanadium compounds produced sustained or oscillatory $Ca^{2+}$ elevations; in nominally $Ca^{2+}$-free medium, a transient $Ca^{2+}$ rise was generated. Vanadate-induced $Ca^{2+}$ signaling was blocked by heparin, a competitive inhibitor of the 1,4,5-inositol trisphosphate ($IP_3$) receptor, suggesting that $Ca^{2+}$ influx is secondary to depletion of $IP_3$-sensitive $Ca^{2+}$ stores. In Jurkat T cells, vanadate also activated the $Ca^{2+}$-dependent transcription factor, NF-AT. Intracellular dialysis with vanadate activated $Ca^{2+}$ influx through $Ca^{2+}$ release-activated $Ca^{2+}$ (CRAC) channels with kinetics comparable to those of dialysis with $IP_3$. Neither phosphatase inhibitors nor nonhydrolyzable nucleotide analogues modified CRAC channel activation. The action of vanadate, but not $IP_3$, was prevented by the thiol-reducing agent DTT. In addition, the activation of CRAC channels by vanadate was mimicked by the thiol-oxidizing agent chloramine T. These results suggest that vanadate enhances $Ca^{2+}$ signaling via thiol oxidation of a proximal element in the signal transduction cascade.** *The Journal of Immunology,* **2000, 164: 679–687.**

The role of $Ca^{2+}$ signaling in the activation of T lymphocytes is well established (1, 2). Binding of the TCR to Ag associated with the MHC initiates a cascade of intracellular signaling that culminates in the production of cytokines and T cell proliferation. Among the proximal signaling steps that take place at the plasma membrane, tyrosine phosphorylation of substrates, including phospholipase C, generates two key second messengers, diacylglycerol, leading to the activation of protein kinase C, and 1,4,5-inositol trisphosphate ($IP_3$),[5] leading to the initiation of the $Ca^{2+}$ signal. The $Ca^{2+}$ signal is sustained by the activation of a specific type of store-operated $Ca^{2+}$ channel in the plasma membrane called the $Ca^{2+}$ release-activated $Ca^{2+}$ (CRAC) channel (1). $Ca^{2+}$ signaling must be oscillatory or sustained at the level of individual cells to activate gene transcription via the NF-AT pathway, leading to cytokine production (3–5).

Department of Physiology and Biophysics, University of California, Irvine, CA 92697

Received for publication July 2, 1999. Accepted for publication November 2, 1999.

The costs of publication of this article were defrayed in part by the payment of page charges. This article must therefore be hereby marked *advertisement* in accordance with 18 U.S.C. Section 1734 solely to indicate this fact.

[1] This work was supported by National Institutes of Health Grants NS14609 and GM41514 (to M.D.C.) and 5T32CA09054 (from the National Cancer Institute, to C.M.F.), and by fellowships from the Alexander von Humboldt Foundation (to C.E. and H.R.).

[2] Current address: Department of Animal Physiology, Institute of Zoology, University of Salzburg, A-5020 Salzburg, Austria.

[3] Current address: Department of Neurophysiology, Humboldt University, Berlin Germany.

[4] Address correspondence and reprint requests to Dr. M. D. Cahalan, Room 285, Irvine Hall, University of California, Irvine, CA 92697-4560. E-mail address: mcahalan@uci.edu

[5] Abbreviations used in this paper: $IP_3$, 1,4,5-inositol trisphosphate; bpV(pic), dipotassium oxodiperoxo (pyridine-2-carboxylato) vanadate (V); $[Ca^{2+}]_i$, intracellular free calcium concentration; CRAC channel, $Ca^{2+}$ release-activated $Ca^{2+}$ channel; $IP_3R$, $IP_3$ receptor; PTK, protein tyrosine kinase; PTP, protein tyrosine phosphatase; RBL cell, rat basophilic leukemia mast cell; TG, thapsigargin; fura-2-AM, fura-2-acetoxymethyl ester.

The level of cellular tyrosine phosphorylation and subsequent activation events are controlled by a balance between phosphorylation and dephosphorylation reactions. Thus, compounds that alter the balance of kinase and phosphatase activity may profoundly influence cellular activation in the immune response. Sodium orthovanadate ($Na_3VO_4$) is a potent inhibitor of protein tyrosine phosphatase (PTPs) and other phosphoryl transfer enzymes (6). In the +5 oxidation state, vanadate adopts a trigonal bipyramidal configuration that mimics the phosphate ion (7). In this configuration, $Na_3VO_4$ competes with the $\gamma$-phosphate of ATP for binding to the active site of the $Na^+,K^+$-ATPase, thus inhibiting the enzyme (8, 9). $Na_3VO_4$ inhibits PTPs by a similar mechanism (reviewed in Refs. 10–12). Formation of a phosphate-thioester bond with a conserved cysteine at the active site of PTPs is critical to the dephosphorylation reaction. $Na_3VO_4$ reversibly displaces phosphate from the active site thiol (13). In addition, thiol oxidation may permanently inactivate PTPs during prolonged treatment of cells with $Na_3VO_4$ (14). Cysteine could be oxidized directly by $Na_3VO_4$ or indirectly following the intracellular formation of pervanadate. Pervandate is a complex mixture of peroxovanadium compounds formed in vitro by mixing $H_2O_2$ and $Na_3VO_4$ (reviewed in Ref. 10). Pervanadate produces an irreversible inhibition of PTPs that can be prevented by preincubation with thiol-reducing agents, suggesting that the effect of pervanadate is mediated by the oxidation of cysteine (15). Although vanadate and pervanadate have been widely used as general inhibitors of PTPs and clearly enhance tyrosine phosphorylation in immune cells (16–20), the effects of vanadium compounds on other cellular targets as a result of their thiol reactivity have not been fully explored.

The modulation of intracellular signaling by vanadium compounds takes on a greater significance because they are being considered as potential therapeutic agents for use in both insulin-dependent and noninsulin-dependent forms of diabetes (21–25). Their insulin-mimetic actions in vivo and in vitro correlate with their ability to inhibit PTPs and induce phosphorylation of the $\beta$



0022-1767/00/$02.00

subunit of the insulin receptor (26–30). Recent studies have shown that concentrations of vanadium compounds that increase glucose transport and normalize blood glucose levels (21, 31, 32) also produce tyrosine phosphorylation and $Ca^{2+}$ mobilization in Jurkat T cells (16, 17, 33) and RBL cells (18). Thus, potential actions by these compounds on the immune system must also be considered.

Previous attempts to characterize the action of vanadate on cells of the immune system have yielded conflicting results. In Jurkat T cells, pervanadate was reported to induce $Ca^{2+}$ influx independent of store release (17). However, in RBL cells pervanadate appeared to release $Ca^{2+}$ from intracellular stores (18). In many cell types, $Ca^{2+}$ influx is coupled to the depletion of intracellular $Ca^{2+}$ stores by a process termed capacitative $Ca^{2+}$ entry (34, 35). In lymphocytes and RBL cells store release leads to CRAC channel activation (36–42). To clarify the mechanisms of action of vanadate, we have investigated its effects on $[Ca^{2+}]_i$ signaling in Jurkat T lymphocytes and RBL cells using single-cell imaging and electrophysiological techniques. Our experiments were designed to show whether the normal $Ca^{2+}$ signaling mechanisms used by cells of the immune system are usurped by vanadate stimulation, whether $Ca^{2+}$ channel activation is direct or secondary to release from $Ca^{2+}$ stores, and whether nonphysiological mechanisms are evoked.

## Materials and Methods

### *Cell culture*

The human leukemia T cell line, Jurkat E6-1, and the rat basophilic leukemia cell line, RBL-2H3, were obtained from American Type Culture Collection (Manassas, VA). Jurkat-NZ cells containing a $\beta$-galactosidase reporter gene construct (*lacZ*) under the control of the NF-AT promoter were derived from the Jurkat subline NZDipA.1.5.22 and have been previously described and characterized (4). Jurkat E6-1 and Jurkat-NZ cells were grown in RPMI 1640 medium containing 10% heat-inactivated FBS, 10 mM HEPES, and 2 mM glutamine. Cells were cultured in 25-ml flasks (Costar, Cambridge, MA) at 37°C in 5% $CO_2$ in a humidified incubator. RBL cells were maintained in Eagle's MEM supplemented with 20% FCS and 2 mM glutamine. RBL cells were plated onto glass coverslips 1–2 days before use.

### *Chemicals*

Thapsigargin (TG) and dipotassium oxodiperoxo (pyridine-2-carboxylato) vanadate (bpV(pic)) were obtained from Alexis Biochemicals (San Diego, CA). 5′-Adenlylimidodiphosphate tetralithium salt was obtained from Roche Molecular Biochemicals (Basel, Switzerland), and adenosine 5′-*o*-(3-thiotriphosphate) tetralithium salt (ATP$\gamma$S) was obtained from Calbiochem (San Diego, CA). All other salts and reagents were obtained from Sigma-Aldrich (St. Louis, MO).

### *Calcium imaging*

Jurkat T cells were loaded with 3 $\mu$M fura-2-AM (Molecular Probes, Eugene, OR) for 30–40 min at room temperature (20–25°C). The cells were then washed three times with RPMI/10% FCS. RBL cells were loaded in medium containing 1 $\mu$M fura-2-AM and 2.5 mM probenecid for 30 min at 37°C in the incubator. These cells were then washed three times with Eagle's MEM containing 2.5 mM probenecid and returned to the incubator for an additional 30 min to complete the hydrolysis of the fura-2 ester. After fura-2 loading, all cells were stored at room temperature in the dark until use. Before imaging, media were exchanged with mammalian Ringer containing: 160 mM NaCl, 4.5 mM KCl, 2 mM $CaCl_2$, 1 mM $MgCl_2$, 10 mM glucose, and 10 mM HEPES (pH 7.4; osmolality, 290–310 mOsm/kg). Illumination was provided by a xenon arc lamp (Carl Zeiss, New York, NY) and transmitted through a filter wheel unit (Lambda 10, Axon Instruments, Foster City, CA) containing 350- and 385-nm excitation filters. The filtered light was reflected by a 400-nm dichroic mirror through a $\times$63 oil immersion objective to illuminate cells. Emitted light above 480 nm was received by an intensified CCD camera (C2400, Hamamatsu Photonics, Bridgewater, NJ), and the video information was relayed to an image processing system (Videoprobe, ETM Systems, Petaluma, CA). Full field-of-view 8-bit images, averaged over 16 frames, were collected at 350- and 385-nm wavelengths. Digitally stored 350/385 ratios were constructed from background-corrected 350- and 385-nm images. Single-cell measurements of $[Ca^{2+}]_i$ were calculated from the 350/385 ratios using the equation of Grynkiewicz et al. (43) and a $K_d$ of 250 nM for fura-2. The minimum 350/385 ratio was measured in single cells after incubation for 10 min in $Ca^{2+}$-free Ringer containing 2 mM EGTA. Maximum ratio values were obtained after perfusion with Ringer containing 10 mM $Ca^{2+}$, 1 $\mu$M TG, and 10 $\mu$M ionomycin.

### *Microinjection*

The sodium salt of low molecular mass heparin (average m.w., 3 kDa; Sigma, St. Louis, MO) was made up to a concentration of 25 mg/ml in a 100 mM KCl solution containing 0.1% tetramethylrhodamine dextran (Molecular Probes). The heparin solution was loaded into prepulled glass capillaries (Femtotip, Eppendorf, Hamburg, Germany). Cell microinjection was performed using a pressure injector (model 5246, Eppendorf) and micromanipulator (model 5171, Eppendorf) as previously described (44). Microinjections were performed 2 h before the calcium imaging experiments.

### *Whole-cell recording*

Membrane currents were measured in Jurkat T cells using the whole-cell configuration of the patch-clamp technique (45, 46). An EPC-9 amplifier (HEKA, Lambrecht, Germany) interfaced to a Macintosh Quadra 700 computer (Apple Computer, Cupertino, CA) was used for pulse application and data recording. Membrane voltages were corrected for liquid junction potentials, and current recordings were corrected for leak and capacitative currents. Patch pipettes were pulled from Accu-fill 90 Micropets (Becton Dickinson, Parsippany, NJ) using a P87 micropipette puller (Sutter Instruments, Novato, CA). Pipettes were coated with Sylgard (Dow Corning, Midland, MI) and heat polished to a final resistances of 2–5 M$\Omega$. Patch-clamp experiments were performed at room temperature (20–25°C). Unless otherwise indicated the membrane currents were filtered at 1.5 kHz. Data analysis was performed using the program Pulse (HEKA, Lambrecht, Germany). During the whole-cell recordings, the membrane potential was held at 0 mV, and the $Ca^{2+}$ current through CRAC channels was measured during 200-ms voltage ramps from $-100$ to $+40$ mV applied at 1-s intervals. The pipette solution contained 128 mM $Cs^+$ aspartate, 12 mM bis(2-aminophenoxy)ethane-*N*,*N*,*N*′,*N*′-tetraacetate (BAPTA), 0.9 mM $CaCl_2$, 3.16 mM $MgCl_2$, and 10 mM HEPES; was titrated to pH 7.2 with CsOH; and had an estimated free $Ca^{2+}$ concentration of 10 nM. The external solution had the following composition: 150 mM $NaMeSO_3$, 20 mM $CaCl_2$, 10 mM glucose, and 10 mM HEPES and was titrated to pH 7.4 with NaOH.

### *The* lacZ *reporter gene assay*

The expression of *lacZ* was measured using a fluorescence assay as previously described (47). In brief, Jurkat-NZ cells were seeded at $1 \times 10^5$ cells/well in 96-well plates containing culture medium alone or with addition of 1 $\mu$M TG or varying concentrations of bpV(pic), each condition in the presence or the absence of 50 nM PMA. The cells were activated in a humidified incubator at 37°C with 5% $CO_2$ for 10 h, then lysed and incubated with 3 mM 4-methylumbelliferyl $\beta$-D-galactopyranoside (Molecular Probes). The fluorescence signal measured in a multiwell plate reader (CytoFluor Series 4000, Perspective Biosystems, Framingham, MA; 400 nm excitation, 505 nm emission) is proportional to *lacZ* activity driven by the NF-AT pathway.

### *Data analysis*

Numerical values for single-cell $[Ca^{2+}]_i$ traces were analyzed with Origin (Microcal, Northhampton, MA). Statistical analysis was performed on data sets using Excel v5.0 (Microsoft, Redmond, WA). Data are reported as the mean $\pm$ SD. Multisample hypotheses were tested using a single-factor ANOVA and performing a Dunnett's test to determine the significance of differences from control values. Data were considered statistically different at $p < 0.05$.

## Results

### *The bpV(pic) activates $Ca^{2+}$ signaling in Jurkat T lymphocytes and RBL-2H3 mast cells*

Previous studies (17, 18) demonstrated that application of peroxovanadium compounds increased $[Ca^{2+}]_i$ in both RBL cells and Jurkat T cells. However, different mechanisms have been postulated for the $Ca^{2+}$ increase in each cell type. These differences may have been due to cell-specific effects of pervanadate or to different mixtures of peroxyvanadium compounds being used each study. To test the hypothesis that peroxyvanadium compounds act by a

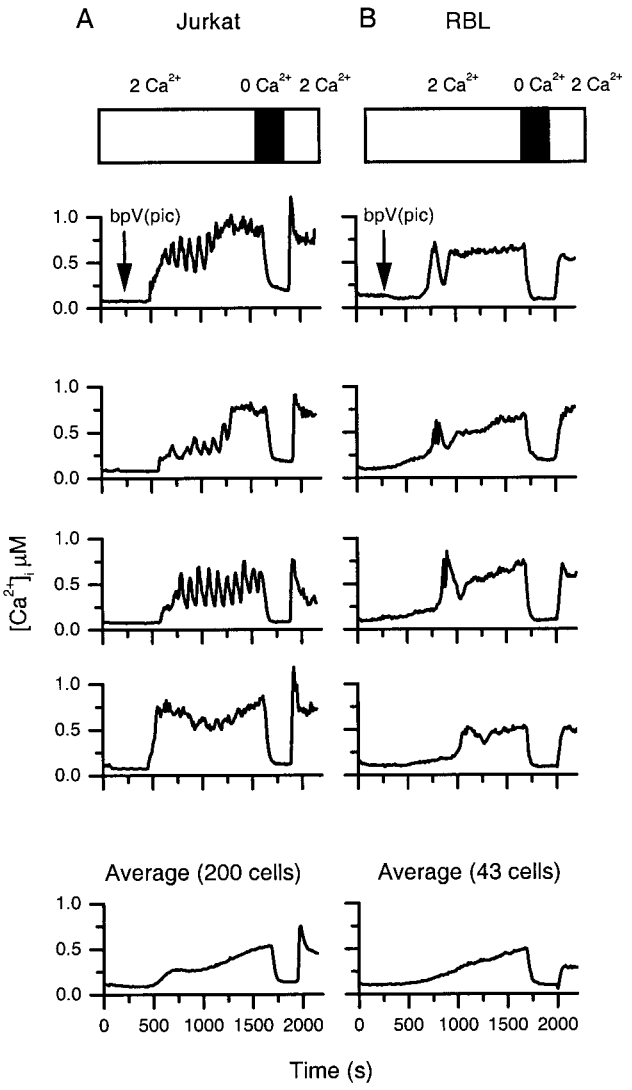


**FIGURE 1.** The $[Ca^{2+}]_i$ signaling induced by bpV(pic). $[Ca^{2+}]_i$ was measured as described in *Materials and Methods* in Jurkat T cells (*A*) and RBL cells (*B*). Resting $[Ca^{2+}]_i$ was determined in mammalian Ringer. At 300 s, 200 $\mu$M bpV(pic) was added to the Ringer (*arrow*). As illustrated (application bar), the $Ca^{2+}$ concentration of the Ringer was varied between 2 mM (2 $Ca^{2+}$) and nominally $Ca^{2+}$ free (0 $Ca^{2+}$). Traces for four representative cells (*top four graphs*) and the average of all cells within the field of view (*bottom graph*) are shown.

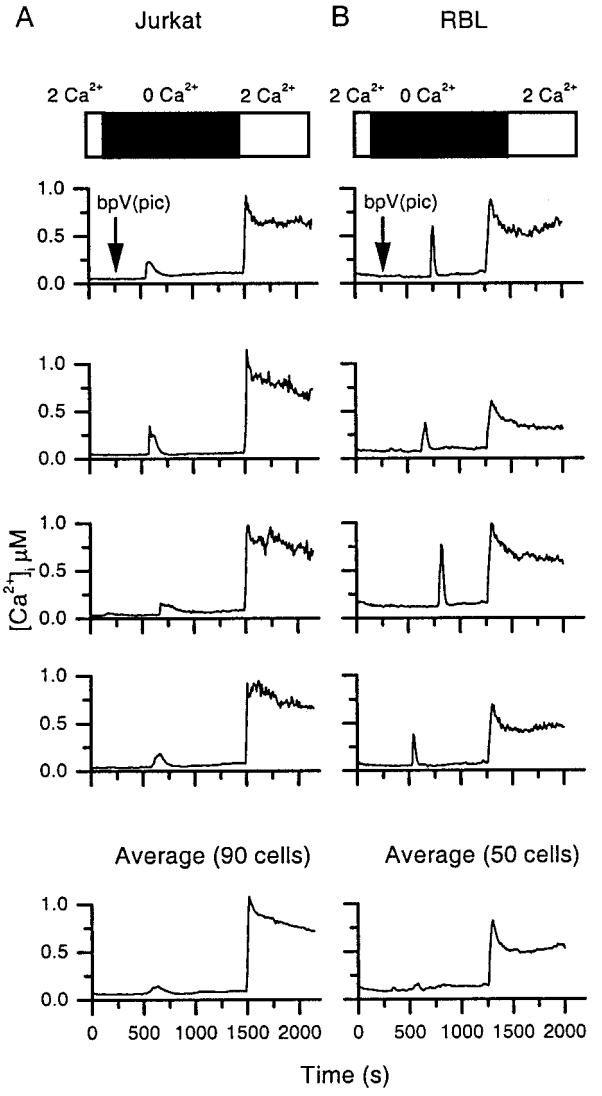


**FIGURE 2.** The bpV(pic) releases $Ca^{2+}$ from intracellular stores. Jurkat T cells (*A*) or RBL cells (*B*) were stimulated with 200 $\mu$M bpV(pic) (*arrow*) in the absence of extracellular calcium. Extracellular $Ca^{2+}$ was varied between 2 mM and nominally $Ca^{2+}$ free (application bar). The $[Ca^{2+}]_i$ is shown for four representative cells (*top four graphs*) and the average of all cells within the field of view (*bottom graph*).

similar mechanism on T cells and mast cells we tested the effects of the cell-permeant peroxyvanadium compound, bpV(pic) on Jurkat T cells and RBL mast cells. When exposed to bpV(pic) (200 $\mu$M) in the presence of extracellular $Ca^{2+}$, most Jurkat T cells (80 $\pm$ 10%) responded after a variable delay with an abrupt increase in $[Ca^{2+}]_i$. In the majority of responding cells the initial rise in $[Ca^{2+}]_i$ was followed by slow oscillations with a 73 $\pm$ 4-s period and a peak $[Ca^{2+}]_i$ near 700 nM (Fig. 1*A*). The average $Ca^{2+}$ response from all observed cells (Fig. 1*A*, *bottom graph*) rose smoothly from the resting level of 66 $\pm$ 41 nM to a plateau of 488 $\pm$ 210 nM. This population response reflects the asynchronous $Ca^{2+}$ oscillations in single cells and the fact that the average includes nonresponding cells. Our data confirm earlier observations that peroxovanadium compounds increase $[Ca^{2+}]_i$ in Jurkat T cells (16, 17) and reveal at the single-cell level that bpV(pic) can produce $Ca^{2+}$ oscillations analogous to those produced during Ag presentation (48). Extracellular $Ca^{2+}$ is required to maintain the bpV(pic)-induced oscillations, because exchanging the bath solution with nominally $Ca^{2+}$-free Ringer's solution rapidly and reversibly terminated the oscillations (Fig. 1*A*, *application bar*).

Treatment of RBL cells with pervanadate results in $Ca^{2+}$ responses that vary with the peroxovanadium compounds formed in the mixture (18). Using bpV(pic), we characterized the effects of a single form of peroxovanadate on RBL cells. The average response of RBL cells to 200 $\mu$M bpV(pic) closely resembled that of the Jurkat T cells (Fig. 1*B*). The $[Ca^{2+}]_i$ began to increase 200 s after the application of bpV(pic) and gradually approached a plateau of 500 $\pm$ 170 nM after an additional 1200 s. The sustained $Ca^{2+}$ plateau required $Ca^{2+}$ influx, because $[Ca^{2+}]_i$ returned to baseline during perfusion with nominally $Ca^{2+}$-free Ringer's solution (Fig. 1*B*, application bar). Examination of the responses of individual cells revealed that RBL cells were less prone to oscillate than the Jurkat T cells and appeared to have a biphasic response to bpV(pic) consisting of an initial transient $[Ca^{2+}]_i$ rise followed by a secondary $[Ca^{2+}]_i$ increase to a plateau.

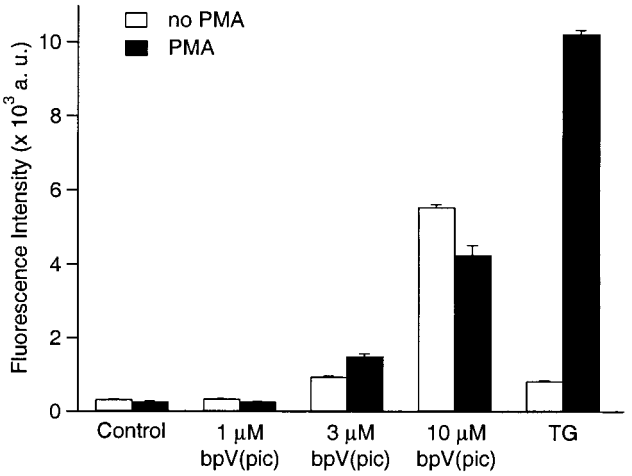


**FIGURE 3.** The bpV(pic) activates NF-AT in Jurkat T cells. The NF-AT-mediated gene expression in Jurkat-NZ cells was measured in a multiwell fluorescence plate reader using a 4-methylumbelliferyl β-D-galactopyranoside assay as described in *Materials and Methods*. Fluorescence measurements were made on unstimulated cells (Control) or cells stimulated for10 h by the indicated treatment, with or without 50 nM PMA. The *lacZ* expression is plotted in arbitrary fluorescence units (a.u.); each bar represents the mean ± SD of six samples. Similar results were obtained in four repetitions.

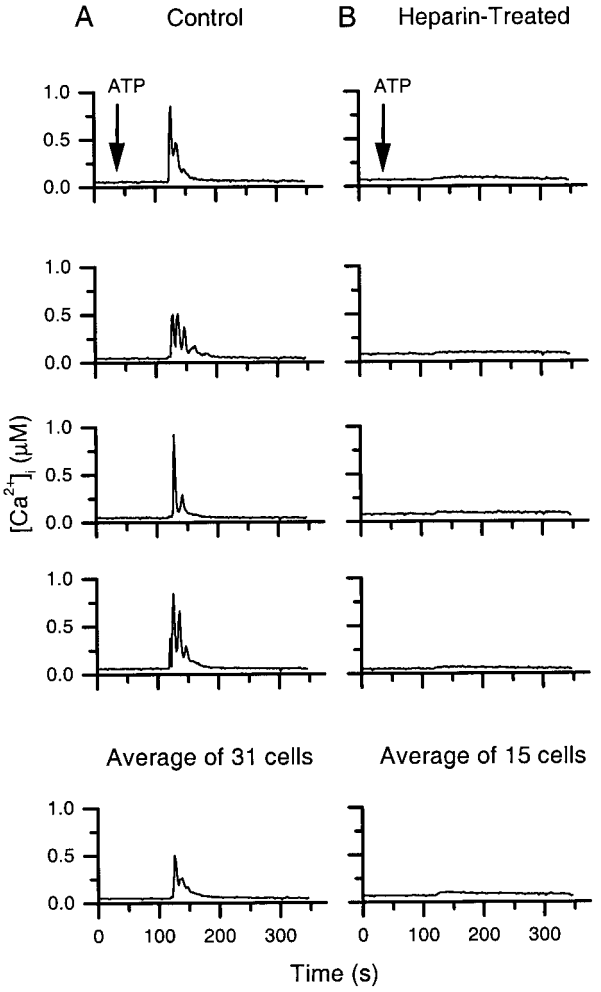


**FIGURE 4.** Heparin blocks $[Ca^{2+}]_i$ signaling elicited by purinergic stimulation. Before $Ca^{2+}$ measurements, single RBL cells were microinjected with heparin (Heparin-injected) or were left uninjected (Control). The $[Ca^{2+}]_i$ was measured in mammalian Ringer at rest and following the application of 4 μM ATP (arrow). For each condition, $[Ca^{2+}]_i$ is shown for four representative cells (*top four graphs*) and the average of all cells within the field of view (*bottom graph*)

*Treatment with bpV(pic) releases $Ca^{2+}$ from intracellular stores*

To separate the contributions of $Ca^{2+}$ release and $Ca^{2+}$ influx, we applied bpV(pic) in nominally $Ca^{2+}$-free Ringer's solution. For both Jurkat T and RBL cells, single-cell records show that application of bpV(pic) elicited an abrupt $[Ca^{2+}]_i$ transient following a variable delay averaging 257 ± 177 s in Jurkat T cells and 579 ± 260 s in RBL cells (Fig. 2). In the averaged response (Fig. 2, *bottom graphs*), the $Ca^{2+}$ transient appeared blunted due to the variation in response times between cells. In some experiments, the variation in latency resulted in the masking of initial $[Ca^{2+}]_i$ transients in the averaged response. However, analysis of the single-cell responses clearly showed that bpV(pic) releases $Ca^{2+}$ from intracellular stores. $Ca^{2+}$ readdition to $Ca^{2+}$-depleted cells caused $[Ca^{2+}]_i$ to increase rapidly to a plateau level (750 ± 40 nM in Jurkat T cells and 530 ± 140 nM in RBL cells). Thus, bpV(pic) appears to release $Ca^{2+}$ from intracellular stores and induce capacitative $Ca^{2+}$ influx. To determine the extent of $Ca^{2+}$ store depletion by bpV(pic), we probed for residual $Ca^{2+}$ in the intracellular stores with TG, a specific inhibitor of the microsomal $Ca^{2+}$-ATPase that depletes $Ca^{2+}$ stores in the endoplasmic reticulum. When TG (1 μM) is applied alone in nominally $Ca^{2+}$-free Ringer's solution, it normally produces a rapid and complete emptying of the endoplasmic $Ca^{2+}$ stores, resulting in a $Ca^{2+}$ transient (49). When applied after perfusion with bpV(pic) in nominally $Ca^{2+}$-free Ringer, TG could not elicit a $Ca^{2+}$ transient (data not shown), indicating that bpV(pic) had completely depleted the TG-sensitive $Ca^{2+}$ store.

*The NF-AT-driven gene expression is induced by bpV(pic)*

To assess the long term effects of vanadate treatment, we monitored transcriptional activation of the $Ca^{2+}$-sensitive transcription factor, NF-AT. Jurkat-NZ cells contain a reporter construct in which the β-galactosidase gene (*lacZ*) is driven by a triple, tandem repeat of the NF-AT binding element found in the T cell IL-2 promoter. When Jurkat-NZ cells are activated, the translocation of NF-AT to the nucleus causes a dramatic increase in β-galactosidase production that can be assessed by fluorogenic substrates (4). Stimulation of Jurkat-NZ cells with PMA and TG caused a large increase in NF-AT activity, whereas PMA or TG alone had little effect (Fig. 3). Parallel experiments with bpV(pic) yielded a smaller, but still significant, increase in NF-AT activity over that in untreated cells regardless of the presence of PMA (Fig. 3). The ability of vanadate to induce NF-AT activity in the absence of PMA contrasts with the PMA requirement for gene expression triggered by TG or ionomycin (4, 50). These results suggest that vanadate may also act to induce PKC activity.

*Microinjected heparin blocks the release of $Ca^{2+}$ from $IP_3$-dependent intracellular $Ca^{2+}$ stores by bpV(pic)*

If the effect of bpV(pic) on $[Ca^{2+}]_i$ requires $IP_3$-evoked $Ca^{2+}$ release, blockade of the $IP_3$ receptor ($IP_3R$) with the competitive antagonist heparin (51) should prevent the action of bpV(pic). On the other hand, if vanadate directly activates $Ca^{2+}$ influx, as suggested previously (17), heparin should be without effect. To test the efficacy of heparin microinjection, we made use of the calcium response in RBL cells produced by P2 purinergic receptor stimulation (52). RBL cells were stimulated with the P2 receptor agonist ATP (10 μM) in the presence and the absence of microinjected

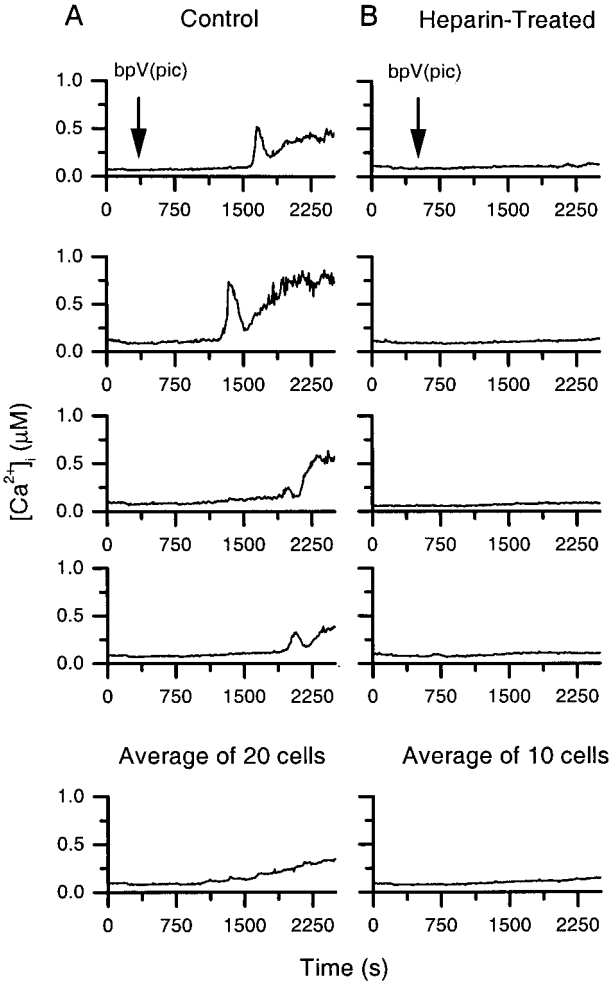


**FIGURE 5.** Heparin blocks $[Ca]_i$ signaling induced by bpV(pic). As described in Fig. 4, $[Ca^{2+}]_i$ was measured in control and heparin-injected RBL cells in mammalian Ringer before and after the application of 200 $\mu$M bpV(pic) (arrow). For each condition, $[Ca^{2+}]_i$ is shown for four representative cells (*top four graphs*) and the average of all cells within the field of view (*bottom graph*).

low m.w. heparin. Fig. 4*A* shows that purinergic stimulation produces an abrupt rise in $[Ca^{2+}]_i$ and several oscillations before $[Ca^{2+}]_i$ returns to baseline levels. As expected, heparin-injected RBL cells (Fig. 4*B*) did not respond to purinergic stimulation. Stimulation by bpV(pic) was inhibited by heparin injection (Fig. 5). Both the initial $Ca^{2+}$ transient and the delayed $Ca^{2+}$ plateau were completely blocked. In contrast, heparin preinjection did not inhibit $Ca^{2+}$ responses evoked by TG or ionomycin (data not shown), demonstrating that heparin did not interfere directly with CRAC channel function. Microinjection with control dextrans had no effect on the $Ca^{2+}$ response to bpV(pic). We conclude that both transient and sustained bpV(pic)-mediated $Ca^{2+}$ signals require $IP_3$-dependent release of $Ca^{2+}$.

### *Vanadate, bpV(pic), and $IP_3$ enhance the rate of activation of CRAC channels*

In Jurkat T cells, depletion of intracellular $Ca^{2+}$ stores results in the opening of CRAC channels and $Ca^{2+}$ influx. During passive store depletion by intracellular dialysis with heavily buffered low $Ca^{2+}$ solutions, an initial lag period was followed by the development of inward $Ca^{2+}$ current through CRAC channels (Fig. 6). These currents exhibit inward rectification, voltage-independent

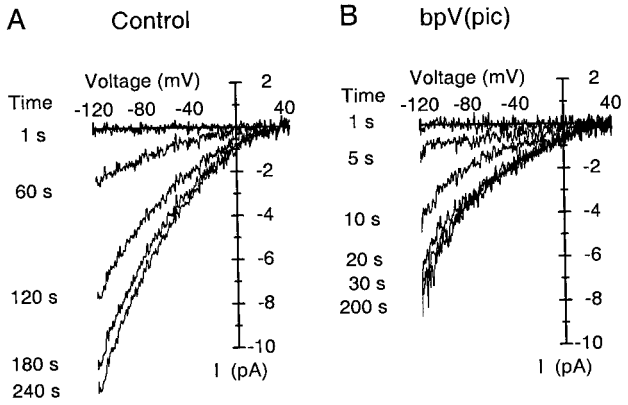


**FIGURE 6.** The bpV(pic) accelerates activation of CRAC channels in Jurkat T cells. Whole-cell patch clamp recordings of $Ca^{2+}$ currents through CRAC channels were made during passive store depletion alone (*A*) or during intracellular dialysis with 10 $\mu$M bpV(pic) (*B*). Voltage clamp protocol: 200-ms ramps from −120 to +40 mV were taken from a holding potential of 0 mV at intervals of 1 s. Currents during ramps taken before CRAC current induction and after maximal activation are shown. Currents from the first five ramps obtained after beginning whole-cell recording were averaged, and the average was subtracted from the remaining records to eliminate leak currents. The time after establishing the whole-cell patch clamp configuration is indicated to the *left* of each current-voltage plot.

gating, and a reversal potential beyond +40 mV. Inclusion of bpV(pic) in the pipette solution accelerated the activation of the CRAC currents without altering their rectification or reversal potential (Fig. 6). Using the amplitude of the current at −80 mV, we compared the effects of bpV(pic) and vanadate with that of $IP_3$ on the activation of CRAC currents (Fig. 7). When the channels were activated by passive store depletion alone, the current reached its maximum ($-1.18 \pm 0.6$ pA/pF) within 260 s ($t_{1/2} = 122 \pm 48$ s; Fig. 7*A* and Table I). Addition of $IP_3$ (10 $\mu$M) to the intracellular

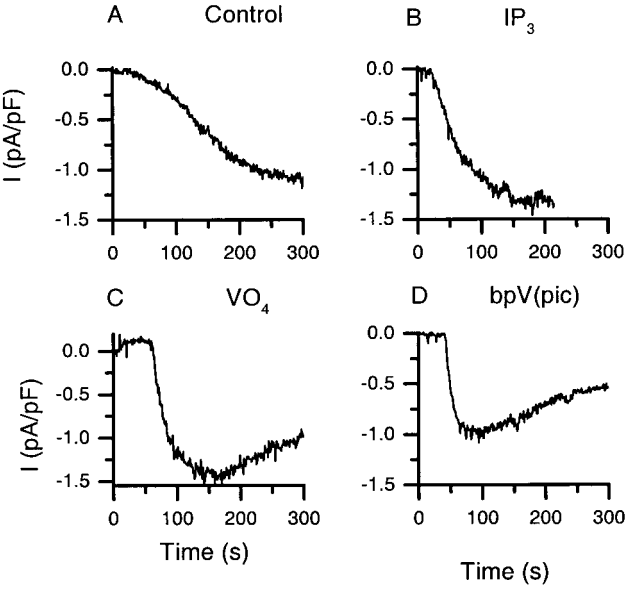


**FIGURE 7.** Time course of CRAC current activation. Whole-cell recordings of $Ca^{2+}$ currents through CRAC channels were made in Jurkat T cells during passive store depletion (*A*) or during intracellular dialysis with 10 $\mu$M $IP_3$ (*B*), 10 $\mu$M $Na_3VO_4$ (*C*), or 10 $\mu$M bpV(pic) (*D*). Currents were recorded as described in Fig. 6, and the CRAC current density at −80 mV is shown from time that the whole-cell patch clamp configuration was established ($t = 0$).

Table I. *Effects of vanadium compounds, thiol-reactive agents and nucleotide substitution on CRAC channel activation*[a]

| | Current Density (pA/pF) | Activation $t_{1/2}$ (s) |
|---|---|---|
| Control | 1.18 ± 0.6 (55) | 122 ± 48 (47) |
| $IP_3$ (10 $\mu$M) | 1.12 ± 0.2 (9) | 14 ± 7 (9)[b] |
| bpV(pic) (10 $\mu$M) | 0.89 ± 0.2 (9) | 14 ± 5 (9)[b] |
| $VO_4$ (10 $\mu$M) | 0.81 ± 0.1 (8) | 29 ± 18 (8)[b] |
| Calyculin A (0.1 $\mu$M) | 0.92 ± 0.4 (8) | 121 ± 38 (8) |
| Okadaic acid (0.5 $\mu$M) | 0.91 ± 0.6 (12) | 111 ± 34 (7) |
| AMP-PNP (5 mM) | 0.91 ± 0.2 (7) | 126 ± 27 (8) |
| ATP$\gamma$S (5 mM) | 0.90 ± 0.4 (4) | 125 ± 31 (4) |
| $V0_4$ (10 $\mu$M) + DTT (5 mM) | 1.40 ± 0.4 (9) | 119 ± 55 (9) |
| $IP_3$ (10 $\mu$M) + DTT (5 mM) | 0.97 ± 0.4 (5) | 16 ± 9 (5)[b] |
| Chloramine T (500 $\mu$M) | 1.32 ± 0.1 (5) | 36 ± 23 (5)[b] |

[a] During whole-cell recording, CRAC channel currents were measured in Jurkat T cells in response to 200-ms voltage ramps from −120 mV to 40 mV, applied at 1-s intervals from a holding potential of 0 mV. The indicated reagents were added by intracellular dialysis from the pipette. The amplitude of the current was determined at −80 mV, and the time to half maximal activation ($t_{1/2}$) was measured. Currents were divided by membrane capacitance to calculate the current density. Data are presented as mean ± SD with number of cells studied.

[b] Value significantly different from control; $p < 0$ 01.

solution accelerated activation of the CRAC current, reducing the $t_{1/2}$ of activation to 14 ± 7 s, but did not alter the final amplitude of the current (Fig. 7*B* and Table I). Dialysis of the cell with solutions containing bpV(pic) or $Na_3VO_4$ (10 $\mu$M) also accelerated the activation of CRAC channels (Fig. 7, *C* and *D*) reducing the $t_{1/2}$ to 14 ± 5 and 29 ± 18 s, respectively. Thus, the enhanced rate of activation of CRAC currents by $Na_3VO_4$ and bpV(pic) mimicked the well-studied effects of $IP_3$ on CRAC currents.

### *The effect of $Na_3VO_4$ on the rate of CRAC channel activation does not require ATP*

The actions of $Na_3VO_4$ and bpV(pic) on CRAC channels could result from increased tyrosine phosphorylation secondary to phosphatase inhibition. We used nucleotide replacement to test whether the effects of $NaVO_4$ could be duplicated by changes in the level of cellular phosphorylation. ATP$\gamma$S is an ATP analogue that is readily used by kinases (53–56). When the thiophosphoryl group from ATP$\gamma$S is transferred to a protein, the resulting bond is resistant to the action of phosphatases. Therefore, nucleotide substitution of ATP$\gamma$S for ATP should mimic the effects of inhibiting intracellular phosphatases. Intracellular dialysis with 5 mM ATP$\gamma$S did not alter the amplitude or rate of activation of CRAC currents (Table I). Furthermore, intracellular dialysis with adenylimidodiphosphate tetralithium salt (5 mM), a nonhydrolyzable analogue of ATP that should reduce protein phosphorylation, did not reduce the rate of CRAC channel activation. In addition, the serine phosphatase inhibitors okadaic acid and calyculin did not increase the rate of CRAC channel activation (Table I). Thus, treatments that shift the phosphorylation status of cellular proteins did not duplicate the effects of vanadate on CRAC channels.

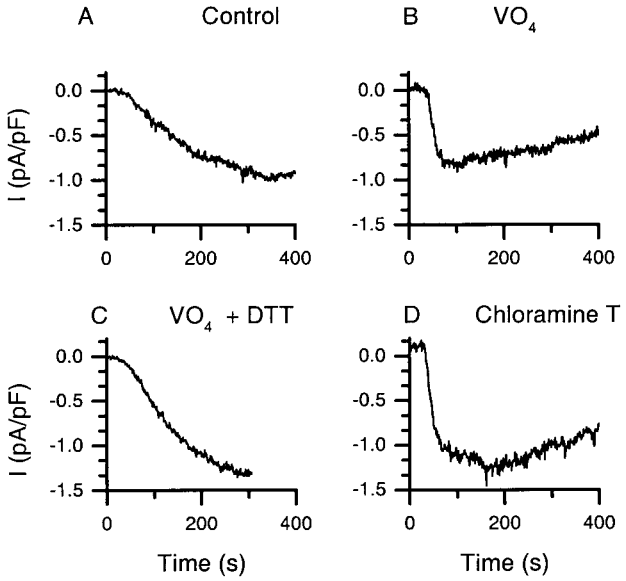


**FIGURE 8.** Dithiothreitol blocks and chloramine T mimics vanadate-induced activation of CRAC currents. Whole-cell patch-clamp recordings of the CRAC currents in Jurkat T cells were measured at −80 mV during passive store depletion (*A*), during intracellular dialysis with 10 $\mu$M $Na_3VO_4$ (*B*), during intracellular dialysis with 10 $\mu$M $Na_3VO_4$ with 1 mM DTT in the pipette and bath solutions (*C*), or during intracellular dialysis with 500 $\mu$M chloramine T (*D*). Currents were recorded as described in Fig. 6 and are shown from time that the whole-cell patch clamp configuration was established ($t = 0$).

### *Thiol oxidation mediates the effects of vanadate on CRAC current activation*

To determine whether the effects of vanadate on CRAC currents are mediated by interaction with cysteine residues, we tested whether the action of $Na_3VO_4$ could be prevented by the thiol-reducing agent DTT. Fig. 8, *A–C*, shows that DTT (5 mM; in pipette and bath) prevented the activation of CRAC currents by $Na_3VO_4$ (10 $\mu$M). Comparison of rates of activation shows that DTT can prevent activation of CRAC currents by $Na_3VO_4$, but not $IP_3$ (Table I). To test whether thiol oxidation alone could enhance the activation of CRAC channels, we included chloramine T, an agent that selectively oxidizes methionine and cysteine residues (57), in the intracellular solution. The rate of activation of CRAC channels was enhanced by chloramine T with respect to activation during passive store depletion (Fig. 8, *C* and *D*, and Table I). These data demonstrate that intracellular dialysis with vanadate or chloramine T produces an increased rate of activation of CRAC currents. Shifting the intracellular redox state to a more reducing environment eliminates the activity of both compounds, suggesting that the effects of vanadate and chloramine T are mediated by thiol oxidation. We further evaluated the hypothesis that chloramine T and vanadate act via the same mechanism. Fig. 9*A* shows that chloramine T, like pbV(pic) (Fig. 5), produces a gradual rise in $[Ca^{2+}]_i$ from baseline to micromolar levels that was inhibited by preinjection with heparin. Thus, $Ca^{2+}$ signaling induced by either

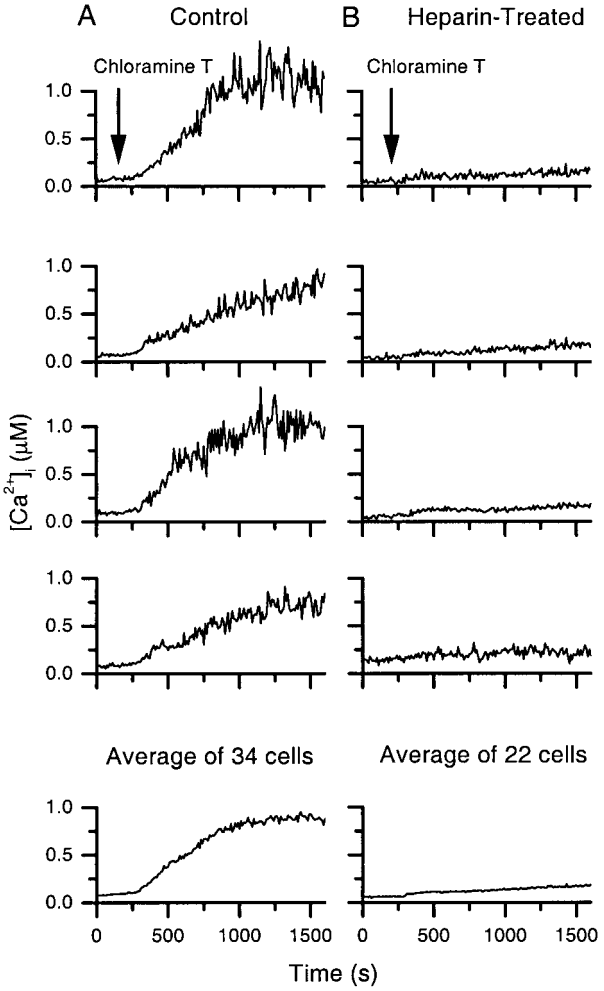


**FIGURE 9.** Chloramine T and bpV(pic) induce calcium signaling in RBL 2H3 cells by similar mechanisms. As shown in Fig. 5 for bpV(pic), heparin blocks $[Ca^{2+}]_i$ signaling elicited by chloramine T. Before $Ca^{2+}$ measurements, single RBL cells were microinjected with heparin (Heparin-injected*)* or were left uninjected (Control*)*. The $[Ca^{2+}]_i$ was measured in mammalian Ringer's solutin and following the application of 50 $\mu$M chloramine T (arrow*)*. For each condition, $[Ca^{2+}]_i$ is shown for four representative cells (*top four graphs*) and the average of all cells within the field of view (*bottom graph*).

vanadate or chloramine T requires $IP_3$-dependent intracellular $Ca^{2+}$ release.

## Discussion

The data presented above demonstrate that treatment with the peroxovanadium compound, bpV(pic), induces $Ca^{2+}$ release from intracellular stores and $Ca^{2+}$ entry in Jurkat T lymphocytes and RBL cells. Single-cell $[Ca^{2+}]_i$ imaging revealed oscillations as well as sustained $[Ca^{2+}]_i$ signals when extracellular $Ca^{2+}$ was present. In the absence of extracellular $Ca^{2+}$, $Ca^{2+}$ release transients evoked by vanadate led to complete depletion of the TG-sensitive store. Heparin, which blocks the association of $IP_3$ with its receptor, blocked bpV(pic)-induced $Ca^{2+}$ signaling. Remarkably, intracellular dialysis with bpV(pic) or $Na_3VO_4$ activated CRAC channels as rapidly as dialysis with $IP_3$. CRAC channel activation by vanadium compounds was prevented by incubation with the thiol-reducing agent DTT and was mimicked by the thiol oxidant chloramine T, suggesting that a redox reaction contributes to their mechanism of action. $Ca^{2+}$ signaling induced by bpV(pic) resulted in downstream effects on gene expression by activating the transcription factor, NF-AT, without a requirement for costimulation by addition of PMA.

Where does vanadate act to promote $Ca^{2+}$ signaling? In principle, vanadate could produce $Ca^{2+}$ influx directly by activating $Ca^{2+}$ channels in the plasma membrane or indirectly by releasing $Ca^{2+}$ from intracellular stores. The CRAC activation by vanadate was extremely rapid (Table I), suggesting that vanadate bypasses the membrane-delimited, rate-limiting steps in $Ca^{2+}$ influx activation following TCR engagement. However, rapid kinetics alone do not indicate that CRAC channels are directly affected by vanadate. Our data clearly demonstrate that vanadate elicits the release of $Ca^{2+}$ from intracellular stores in both RBL and Jurkat T cells (Fig. 2). Furthermore, heparin inhibited vanadate-induced $Ca^{2+}$ entry in RBL cells (Fig. 5), indicating that $Ca^{2+}$ entry is secondary to intracellular $Ca^{2+}$ store depletion and requires the binding of $IP_3$ to its receptor in the endoplasmic reticulum. Finally, currents activated by vanadate were indistinguishable in every characteristic from those activated by dialysis with $IP_3$ or by passive $Ca^{2+}$ store depletion (Fig. 6). Taken together, our results eliminate the possibility that vanadate produces $Ca^{2+}$ influx by direct activation of CRAC channels or any other $Ca^{2+}$ influx mechanism. These data are consistent with earlier studies showing pervanadate-induced $Ca^{2+}$ entry secondary to store release in single RBL cells (18), but conflict with results in Jurkat T cells suggesting that pervanadate directly activates membrane $Ca^{2+}$ channels (17). The latter conclusion was drawn when a rise in $[Ca^{2+}]_i$ was not observed in the absence of extracellular $Ca^{2+}$. However, that study was performed on cell suspensions using a spectrophotometer in which the average $Ca^{2+}$ response from many cells was sampled simultaneously. Our results using video imaging of individual cells show that $Ca^{2+}$ transients occur asynchronously following treatment with bpV(pic). Small transients in the absence of extracellular $Ca^{2+}$ would be missed in population studies (see, for example, Fig. 2*B*). Therefore, we conclude that vanadate induces $Ca^{2+}$ influx secondarily to promoting $IP_3$ production and $Ca^{2+}$ store release, consistent with previous results demonstrating increased PLC$\gamma$ activity and higher cytosolic $IP_3$ levels in intact cells (16, 18).

How does vanadate act chemically inside the cell to promote $Ca^{2+}$ signaling? Vanadate and bpV(pic) are multifunctional reagents that can interact with a number of cellular components in two primary modes of action: 1) mimicking the transition state complex formed by the phosphate ion during phosphoryl transfer reactions; and 2) directly oxidizing cysteine thiols (6). Although $Na_3VO_4$ does not shift the total cellular redox state in lymphocytes, which would appear to emphasize the importance of the first mechanism (19), measurements of the total cellular redox state principally assess the status of nonprotein thiols; thus, the selective oxidation of active site cysteines may not be reflected in those experiments. In fact, a number of studies demonstrate that thiol oxidation plays an important role in the mechanism by which vanadium compounds inhibit PTPs. First, inactivation of PTP1B by vanadium compounds is prevented, but not reversed, by the reducing agent DTT (15). Second, pervanadate directly oxidizes the active site cysteine to cysteic acid in PTP1B (15). Third, $Na_3VO_4$ and pervanadate oxidize cysteine sulfhydryls (58). Other agents that cause thiol oxidation, such as thimerosal, have been reported to enhance $Ca^{2+}$ release from intracellular stores through direct interaction with the $IP_3R$ (59–61). Thimerosal was shown to increase both the single-channel conductance and the mean open time of the reconstituted $Ca^{2+}$ release channel (62). In addition, thimerosal-induced $Ca^{2+}$ influx has been linked to the release of $Ca^{2+}$ from intracellular stores and the activation of CRAC channels in the plasma membrane of RBL-2H3 cells (63). Our data

show that chloramine T mimics and DTT reverses the activation of CRAC channels by $Na_3VO_4$ and bpV(pic) (Figs. 8 and 9). Thus, our results favor oxidation as vanadate's mode of action. The primary target must be more proximal than the $IP_3$ receptor, because heparin blocks bpV(pic)-induced $Ca^{2+}$ signaling. Furthermore, vanadate-induced gene expression did not require the presence of phorbol ester (Fig. 3), suggesting a direct action of vanadate on PLC$\gamma$ to generate adequate diacylglycerol for PKC stimulation. Additional effects that might potentiate activity of the $IP_3R$ activity are not excluded.

Of the myriad of cellular actions demonstrated with vanadium compounds, their insulin-mimetic effects have garnered the most clinical interest. Micromolar concentrations of vanadate and peroxovanadium compounds stimulate hexose uptake, glucose oxidation, and lipogenesis in vivo and in vitro (26–28, 31, 64). Clinical trials demonstrating that sodium metavanadate and vanadyl sulfate improve insulin sensitivity and fasting blood glucose levels have led to suggestions for use of these agents in adjunctive therapy in diabetes (22–25). The clinically applied forms of vanadate have been shown to interconvert within the cell to the +5 oxidation state and to pervandate depending upon the intracellular redox state (reviewed in Refs. 10, 11, and 65). Thus, the effects of vanadate on $Ca^{2+}$ signaling may contribute to the insulin-mimetic properties of these compounds. Unfortunately, beyond their beneficial metabolic effects, long term mitogenic and potentially tumorigenic effects of vanadium compounds must be considered (reviewed in Ref. 60). When applied to lymphocytes at clinically relevant concentrations, vanadium compounds mimic receptor-mediated activation. Our data show that bpV(pic) activates NF-AT-dependent gene expression in Jurkat T cells. Previous reports have demonstrated that peroxyvanadate compounds activate c-Jun and c-Fos and induce nuclear translocation of NF-$\kappa$B in lymphocytes (17, 19). Recently, peroxovanadium compounds were shown to stimulate HIV-1 production in latently infected cell lines in conjunction with T cell activation (20). Thus, studies of the mechanisms by which vanadium compounds interact with lymphocytes may have relevance to its proposed clinical application and yield new approaches to other diseases of the immune system.

## Acknowledgments

We appreciate the expert technical assistance of Dr. Luette Forrest during this project. The use of the Optical Biology Shared Resource of the Chao Family Comprehensive Cancer Center is gratefully acknowledged.

## References

1. Lewis, R. S., and M. D. Cahalan. 1995. Potassium and calcium channels in lymphocytes. *Annu. Rev. Immunol. 13:623.*
2. Crabtree, G. R., and N. A. Clipstone. 1994. Signal transmission between the plasma membrane and nucleus of T lymphocytes. *Annu. Rev. Biochem. 63:1045.*
3. Negulescu, P. A., N. Shastri, and M. D. Cahalan. 1994. Intracellular calcium dependence of gene expression in single T lymphocytes. *Proc. Natl. Acad. Sci. USA 91:2873.*
4. Fanger, C. M., M. Hoth, G. R. Crabtree, and R. S. Lewis. 1995. Characterization of T cell mutants with defects in capacitative calcium entry: genetic evidence for the physiological roles of CRAC channels. *J. Cell Biol. 131:655.*
5. Timmerman, L. A., N. A. Clipstone, S. N. Ho, J. P. Northrop, and G. R. Crabtree. 1996. Rapid shuttling of NF-AT in discrimination of $Ca^{2+}$ signals and immunosuppression. *Nature 383:837.*
6. Nechay, B. R. 1984. Mechanisms of action of vanadium. *Annu. Rev. Pharmacol. Toxicol. 24:501.*
7. Crans, D. C., and A. S. Tracey. 1998. The chemistry of vanadium in aqueous and nonaqueous solution. In *Vanadium Compounds: Chemistry, Biochemistry, and Therapeutic Applications*. A. S. Tracey and D. C. Crans, eds. American Chemical Society, Washington, DC, p. 2.
8. Cantley, L. C. J., M. D. Resh, and G. Guidotti. 1978. Vanadate inhibits the red cell $Na^+$,$K^+$ ATPase from the cytoplasmic side. *Nature 272:552.*
9. Cantley, L. C. J., L. G. Cantley, and L. Josephson. 1978. A characterization of vanadate interactions with the Na,K-ATPase: mechanistic and regulatory implications. *J. Biol. Chem. 253:7361.*
10. Shaver, A., N. J. Ng, D. A. Hall, and B. I. Posner. 1995. The chemistry of peroxovanadium compounds relevant to insulin mimesis. *Mol. Cell. Biochem. 153:5.*
11. Crans, D. C., M. Mahroof-Tahir, and A. D. Keramidas. 1995. Vanadium chemistry and biochemistry of relevance for use of vanadium compounds as antidiabetic agents. *Mol. Cell. Biochem. 153:17.*
12. Morinville, A., D. Maysinger, and A. Shaver. 1998. From vanadis to atropos: vanadium compounds as pharmacological tools in cell death signalling. *Trends Pharmacol. Sci. 19:452.*
13. Tracey, A. S., and M. J. Gresser. 1990. Vandates as phosphate analogs in biochemistry. In *Vanadium in Biological Systems: Physiology and Biochemistry*. N. D. Chasteen, ed. Kluwer Academic, Dordrecht, p. 63.
14. Pugazhenthi, S., F. Tanha, B. Dahl, and R.L. Khandelwal. 1996. Inhibition of a Src homology 2 domain containing protein tyrosine phosphatase by vanadate in the primary culture of hepatocytes. *Arch. Biochem. Biophys. 335:273.*
15. Huyer, G., S. Liu, J. Kelly, J. Moffat, P. Payette, B. Kennedy, G. Tsaprailis, M. J. Gresser, and C. Ramachandran. 1997. Mechanism of inhibition of protein-tyrosine phosphatases by vanadate and pervanadate. *J. Biol. Chem. 272:843.*
16. Secrist, J. P., L. A. Burns, L. Karnitz, G. A. Koretzky, and R. T. Abraham. 1993. Stimulatory effects of the protein tyrosine phosphatase inhibitor, pervanadate, on T-cell activation events. *J. Biol. Chem. 268:5886.*
17. Imbert, V., J. F. Peyron, F. Farahi, B. Mari, P. Auberger, and B. Rossi. 1994. Induction of tyrosine phosphorylation and T-cell activation by vanadate peroxide, an inhibitor of protein tyrosine phosphatases. *Biochem. J. 297:163.*
18. Teshima, R., H. Ikebuchi, M. Nakanishi, and J. Sawada. 1994. Stimulatory effect of pervanadate on calcium signals and histamine secretion of RBL-2H3 cells. *Biochem. J. 302:867.*
19. Krejsa, C. M., S. G. Nadler, J. M. Esselstyn, T. J. Kavanagh, J. A. Ledbetter, and G. L. Schieven. 1997. Role of oxidative stress in the action of vanadium phosphotyrosine phosphatase inhibitors: redox independent activation of NF-$\kappa$B. *J. Biol. Chem. 272:11541.*
20. Barbeau, B., R. Bernier, N. Dumais, G. Briand, M. Olivier, R. Faure, B. I. Posner, and M. Tremblay. 1997. Activation of HIV-1 long terminal repeat transcription and virus replication via NF-$\kappa$B-dependent and -independent pathways by potent phosphotyrosine phosphatase inhibitors, the peroxovanadium compounds. *J. Biol. Chem. 272:12968.*
21. Goldfine, A. B., D. C. Simonson, F. Folli, M. E. Patti, and C. R. Kahn. 1995. In vivo and in vitro studies of vanadate in human and rodent diabetes mellitus. *Mol. Cell. Biochem. 153:217.*
22. Goldfine, A. B., D. C. Simonson, F. Folli, M. E. Patti, and C. R. Kahn. 1995. Metabolic effects of sodium metavanadate in humans with insulin-dependent and noninsulin-dependent diabetes mellitus in vivo and in vitro studies. *J. Clin. Endocrinol. Metab. 80:3311.*
23. Cohen, N., M. Halberstam, P. Shlimovich, C. J. Chang, H. Shamoon, and L. Rossetti. 1995. Oral vanadyl sulfate improves hepatic and peripheral insulin sensitivity in patients with non-insulin-dependent diabetes mellitus. *J. Clin. Invest. 95:2501.*
24. Halberstam, M., N. Cohen, P. Shlimovich, L. Rossetti, and H. Shamoon. 1996. Oral vanadyl sulfate improves insulin sensitivity in NIDDM but not in obese nondiabetic subjects. *Diabetes 45:659.*
25. Boden, G., X. Chen, J. Ruiz, G. D. van Rossum, and S. Turco. 1996. Effects of vanadyl sulfate on carbohydrate and lipid metabolism in patients with non-insulin-dependent diabetes mellitus. *Metabolism 45:1130.*
26. Kadota, S., I. G. Fantus, G. Deragon, H. J. Guyda, B. Hersh, and B. I. Posner. 1987. Peroxides of vanadium: a novel and potent insulin-mimetic agent which activates the insulin receptor kinase. *Biochem. Biophys. Res. Commun. 147:259.*
27. Fantus, I. G., S. Kadota, G. Deragon, B. Foster, and B. I. Posner. 1989. Pervanadate [peroxides of vanadate] mimics insulin action in rat adipocytes via activation of the insulin receptor tyrosine kinase. *Biochemistry 28:8864.*
28. Bevan, A. P., J. W. Burgess, J. F. Yale, P. G. Drake, D. Lachance, G. Baquiran, A. Shaver, and B. I. Posner. 1995. In vivo insulin mimetic effects of pV compounds: role for tissue targeting in determining potency. *Am. J. Physiol. 268:E60.*
29. Bevan, A. P., P. G. Drake, J. F. Yale, A. Shaver, and B. I. Posner. 1995. Peroxovanadium compounds: biological actions and mechanism of insulin-mimesis. *Mol. Cell. Biochem. 153:49.*
30. Drake, P. G., and B. I. Posner. 1998. Insulin receptor-associated protein tyrosine phosphatases: role in insulin action. *Mol. Cell. Biochem. 182:79.*
31. Eriksson, J. W., P. Leonnroth, B. I. Posner, A. Shaver, C. Wesslau, and U. P. Smith. 1996. A stable peroxovanadium compound with insulin-like action in human fat cells. *Diabetologia 39:235.*
32. Etcheverry, S. B., D. C. Crans, A. D. Keramidas, and A. M. Cortizo. 1997. Insulin-mimetic action of vanadium compounds on osteoblast-like cells in culture. *Arch. Biochem. Biophys. 338:7.*
33. Imbert, V., D. Farahifar, P. Auberger, D. Mary, B. Rossi, and J. F. Peyron. 1996. Stimulation of the T-cell antigen receptor-CD3 complex signaling pathway by the tyrosine phosphatase inhibitor pervanadate is mediated by inhibition of CD45: evidence for two interconnected Lck/Fyn- or zap-70-dependent signaling pathways. *J. Inflamm. 46:65.*
34. Putney, J. J. 1986. A model for receptor-regulated calcium entry. *Cell Calcium 7:1.*
35. Putney, J. J. 1990. Capacitative calcium entry revisited. *Cell Calcium 11:611.*
36. Lewis, R. S., and M. D. Cahalan. 1989. Mitogen-induced oscillations of cytosolic $Ca^{2+}$ and transmembrane $Ca^{2+}$ current in human leukemic T cells. *Cell Regul. 1:99.*
37. Lewis, R. S., and M. D. Cahalan. 1990. Ion channels and signal transduction in lymphocytes. *Annu. Rev. Physiol. 52:415.*

38. Hoth, M., and R. Penner. 1992. Depletion of intracellular calcium stores activates a calcium current in mast cells. *Nature 355:353.*
39. Zweifach, A., and R. S. Lewis. 1993. Mitogen-regulated $Ca^{2+}$ current of T lymphocytes is activated by depletion of intracellular $Ca^{2+}$ stores. *Proc. Natl. Acad. Sci. USA 90:6295.*
40. Hoth, M., and R. Penner. 1993. Calcium release-activated calcium current in rat mast cells. *J. Physiol. 465:359.*
41. Premack, B. A., T. V. McDonald, and P. Gardner. 1994. Activation of $Ca^{2+}$ current in Jurkat T cells following the depletion of $Ca^{2+}$ stores by microsomal $Ca^{2+}$-ATPase inhibitors. *J. Immunol. 152:5226.*
42. Zhang, L., and M. A. McCloskey. 1995. Immunoglobulin E receptor-activated calcium conductance in rat mast cells. *J. Physiol. 483:59.*
43. Grynkiewicz, G., M. Poenie, and R.Y. Tsien. 1985. A new generation of $Ca^{2+}$ indicators with greatly improved fluorescence properties. *J. Biol. Chem. 260: 3440.*
44. Fanger, C. M., S. Ghanshani, N. J. Logsdon, H. Rauer, K. Kalman, J. Zhou, K. Beckingham, K. G. Chandy, M. D. Cahalan, and J. Aiyar. 1999. Calmodulin mediates calcium-dependent activation of the intermediate conductance $K_{Ca}$ channel, IKCa1. *J. Biol. Chem. 274:5754.*
45. Hamill, O. P., A. Marty, E. Neher, B. Sakmann, and F. J. Sigworth. 1981. Improved patch-clamp techniques for high-resolution current recording from cells and cell-free membrane patches. *Pflügers Arch. Eur. J. Physiol. 391:85.*
46. Cahalan, M. D., K. G. Chandy, T. E. DeCoursey, and S. Gupta. 1985. A voltage-gated potassium channel in human T lymphocytes. *J. Physiol. 358:197.*
47. Ehring, G. R., H. H. Kerschbaum, C. Eder, A. L. Neben, C. M. Fanger, R. M. Khoury, P. A. Negulescu, and M. D. Cahalan. 1998. A nongenomic mechanism for progesterone-mediated immunosuppression: inhibition of $K^+$ channels, $Ca^{2+}$ signaling, and gene expression in T lymphocytes. *J. Exp. Med. 188:1593.*
48. Negulescu, P. A., T. B. Krasieva, A. Khan, H. H. Kerschbaum, and M. D. Cahalan. 1996. Polarity of T cell shape, motility, and sensitivity to antigen. *Immunity 4:421.*
49. Thastrup, O., A. P. Dawson, O. Scharff, B. Foder, P. J. Cullen, B. K. Drobak, P. J. Bjerrum, S. B. Christensen, and M. R. Hanley. 1989. Thapsigargin, a novel molecular probe for studying intracellular calcium release and storage. *Agents Actions 27:17.*
50. Fiering, S., J. P. Northrop, G. P. Nolan, P. S. Mattila, G. R. Crabtree, and L. A. Herzenberg. 1990. Single cell assay of a transcription factor reveals a threshold in transcription activated by signals emanating from the T-cell antigen receptor. *Genes Dev 4:1823.*
51. Ghosh, T. K., P. S. Eis, J. M. Mullaney, C. L. Ebert, and D. L. Gill. 1988. Competitive, reversible, and potent antagonism of inositol 1,4,5-trisphosphate-activated calcium release by heparin. *J. Biol. Chem. 263:11075.*
52. Osipchuk, Y. V., and M. D. Cahalan. 1992. Cell-to-cell spread of calcium signals mediated by ATP receptors in mast cells. *Nature 359:241.*
53. Gadsby, D. C., and A. C. Nairn. 1999. Control of CFTR channel gating by phosphorylation and nucleotide hydrolysis. *Physiol. Rev. 79:S77.*
54. Kuhnae, M. R., Z. Zhao, J. Rowles, B. E. Lavan, S. H. Shen, E. H. Fischer, and G. E. Lienhard. 1994. Dephosphorylation of insulin receptor substrate 1 by the tyrosine phosphatase PTP2C. *J. Biol. Chem. 269:15833.*
55. Wagner, P. D., and N. D. Vu. 1989. Thiophosphorylation causes $Ca^{2+}$-independent norepinephrine secretion from permeabilized PC12 cells. *J. Biol. Chem. 264:19614.*
56. Yount, R. G. 1975. ATP analogs. *Adv. Enzymol. 43:1.*
57. Shechter, Y., Y. Burstein, and A. Patchornik. 1975. Selective oxidation of methionine residues in proteins. *Biochemistry 14:4497.*
58. Mikalsen, S. O., and O. Kaalhus. 1998. Properties of pervanadate and permolybdate: connexin43, phosphatase inhibition, and thiol reactivity as model systems. *J. Biol. Chem. 273:10036.*
59. Bird, G. S., G. M. Burgess, and J. J. Putney. 1993. Sulfhydryl reagents and cAMP-dependent kinase increase the sensitivity of the inositol 1,4,5-trisphosphate receptor in hepatocytes. *J. Biol. Chem. 268:17917.*
60. Pintado, E., D. Baquero-Leonis, M. Conde, and F. Sobrino. 1995. Effect of thimerosal and other sulfhydryl reagents on calcium permeability in thymus lymphocytes. *Biochem. Pharmacol. 49:227.*
61. Kaplin, A. I., C. D. Ferris, S. M. Voglmaier, and S. H. Snyder. 1994. Purified reconstituted inositol 1,4,5-trisphosphate receptors: thiol reagents act directly on receptor protein. *J. Biol. Chem. 269:28972.*
62. Thrower, E. C., H. Duclohier, E. J. Lea, G. Molle, and A. P. Dawson. 1996. The inositol 1,4,5-trisphosphate-gated $Ca^{2+}$ channel: effect of the protein thiol reagent thimerosal on channel activity. *Biochem. J. 318:61.*
63. Parekh, A. B., and R. Penner. 1995. Activation of store-operated calcium influx at resting InsP3 levels by sensitization of the InsP3 receptor in rat basophilic leukaemia cells. *J. Physiol. 489:377.*
64. Leonnroth, P., J. W. Eriksson, B. I. Posner, and U. Smith. 1993. Peroxovanadate but not vanadate exerts insulin-like effects in human adipocytes. *Diabetologia 36:113.*
65. Stern, A., X. Yin, S. S. Tsang, A. Davison, and J. Moon. 1993. Vanadium as a modulator of cellular regulatory cascades and oncogene expression. *Biochem. Cell Biol. 71:103.*